JOURNAL OF MATERIALS SCIENCE **37** (2002) 3405 – 3413

On the mechanosorptive effect in porous ceramics

Part II *Effect of heating on alumina*

J. LEPAGE
Laboratoire de Science et Génie des Surfaces, LSGS, UMR 7570 CNRS, Ecole des Mines, Parc de Saurupt, 54042 Nancy Cédex, France
E-mail: lepage@mines.u-nancy.fr

Gibbsite containing alumina samples have been heated up to 1200°C in air. The decomposition of gibbsite and/or the departure of hydroxyls are found to influence the mechanical behaviour of porous alumina in the presence of water to a large extent. Powdered products of gibbsite decomposition first lead to a decrease in the Young's modulus. Sintering then occurs, dominated by the hydroxyl content, to reestablish the initial values. Two mechanical models are presented. In the first one, cohesion of granular solids results from the density of H-bonds inside the solids. In the second one, surface energy effects across grain boundaries dominate the mechanical behaviour. Application to various granular solids is discussed.

1. Introduction

Recently we presented experimental evidences that the interactions between water and solid surfaces are governed by the relative hydrophilic/hydrophobic character of such surfaces [1, 2]. Starting with a given material, variations of the wetting properties of solid surface can be operated along two routes. The first one is surface modification by chemical means, for instance the adsorption of trimethylchlorosilane to replace polar OH groups by non polar $Si(CH_3)_3$ groups on hydroxylated silica [3]. A second and more convenient mean is the dehydroxylation of the surfaces by heating. In the first part of this paper we review some of the published works dealing with the relation between surface modifications and variations in the mechanical properties of solid, then we focus our attention on the heat induced modification of porous solids, taking into account some of our previously published results. The results allow us to present a discussion on the surface forces operative in these systems.

2. Analysis of published works

For a long time it has been recognized that the elastic properties of rocks are governed by flat cracks and more or less spherical pores. Various empirical relations linking the Young's modulus E and the mean porosity Φ have been proposed. The most well known relation

$$E = E_o \exp(-b\Phi) \quad (1)$$

has been shown to represent quite well the changes in Young's modulus during the oxidation of graphite [1]. The exponent b is characteristic of the geometry of the flaw, a large value ($b \sim 6$) indicates flat cracks while a low value ($b \sim 3$) indicates round pores. It is generally admitted that, due to differential coefficients of thermal expansion among the components, heating a heterogeneous material creates thermal stresses that can induce cracks. Young's modulus is then a measurement of the thermal damage imposed to the materials and in this section some of the most relevant papers are reviewed.

The aim of Tourenq *et al.* experiments [4] was to study the capillary forces in flat cracks of large surface to volume ratio. For this purpose they compare the velocity of acoustic waves V (related to the Young's modulus by the relation $E \sim \rho V^2$ where ρ is the specific mass of the material) in the wet (V_w) and in the dry (V_d) conditions. Results on Carrera marble are presented in a V_d versus V_w representation, variations of V_d being obtained by heating at higher and higher temperature, a treatment that is supposed to induce extensive cracking. At low cracking temperatures i.e., high V_d, experimental points are located under the first bissecting line $V_d = V_w$, while they are located above the $V_d = V_w$ line at high cracking temperatures. The $V_d = V_w$ line represents a situation where soaking does not influence the mechanical properties of rocks, $V_d < V_w$ means that the cracks are closed by capillary forces acting in a manner similar to a hydrostatic pressure. $V_w < V_d$ means that water at the cracks weakens the whole system. At high V_d it is expected that the temperature of heating (not indicated in the article) is low and that the surfaces are still hydrophilic. At lower V_d, i.e., higher temperatures of annealing, the hydroxyl concentration at the surfaces is depleted, leading to hydrophobic surfaces with poor wetting properties. A schematic representation

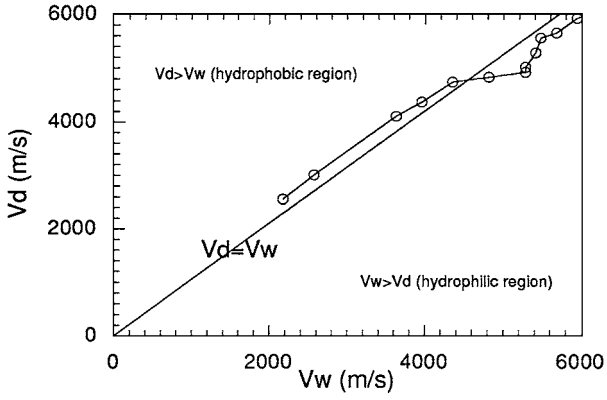

Figure 1 V_d versus V_w representation of Tourenq's experiments.

of Tourenq's results is given on Fig. 1. No results on attenuation were presented in this work.

Morlier [5] used thermal cracking to study water inside rocks. The author concluded that, because of unspecified water-surface interactions, water in cracks is in a solid-like state similar to ice.

The purpose of Clark *et al.* [6] was to look simultaneously at the variations of the damping factor Q^{-1} and of the Young's modulus E on various minerals (quartzite) after heating. Since it is known that cracked rocks have a high damping factor it is expected that thermal cracking raises Q^{-1} and decreases E. They noted that adsorption of water vapour at $p/p_o < 0.1$ leads to a dramatic increase in Q^{-1} while the Young's and shear moduli are only slightly affected. A clear distinction is made between bound water adsorbed at $p/p_o < 0.1$ and free water adsorbed at $p/p_o > 0.1$. On heating the samples up to 675°C a four-fold decrease in the elastic moduli was observed. Furthermore the sensitivity of the mechanical properties toward liquid water soaking was greatly reduced. The damping factor at $p/p_o = 0$ did not depend on the calcination temperature, i.e., on the hydroxyl content of the sample. This proves that on quartzite as well as on Vycor [1] the damping factor can be written

$$Q^{-1} = Q_0^{-1} + k[\mathrm{OH}][\mathrm{H_2O}_b]. \qquad (2)$$

From the above analysis it is clear that Clark's samples contained some hydratable materials, perhaps clay, that underwent dehydration upon heating. Clark's work bears large similarities with ours, however it lacks mass loss studies during calcination. In order to reveal changes in cracking rates she performed water vapour adsorption isotherms that did not reveal changes in surface area. Obviously, water vapour adsorption cannot reveal increases in surfaces area during bake-out at high temperature since this treatment dehydroxylates the surfaces and so reduces water vapour adsorption [7]. In this paper krypton adsorption isotherms at liquid nitrogen temperature have been conducted and, as the initial surface area is low, small relative changes in surface areas are easily detected.

During experiments on Brazilian gabbro, Gregory [8] found that heating at 750°C induced a fourfold decrease in the Young's modulus derived from wave velocity measurements. This lowering was attributed to thermal cracks.

Nonnet *et al.* [9] and Richard *et al.* [10] used also wave velocity measurements to study the variations in Young's modulus of high-alumina containing cement castables at temperatures up to 1600°C. At the same time weight and dimensional changes were recorded and possible phase changes analysed with the help of Synchrotron Radiation-Energy dispersive Diffraction (SR-EDD). On the first heating of a sample, a large drop in E was noticeable at 250°C ($\frac{\Delta E}{E} = -50\%$) while a 5% mass loss occured at that temperature. The authors claimed that, as dehydration proceeds, gibbsite transforms to poorly crystallized alumina leading to increased porosity and poor cohesion between the grains. At temperature annealing higher than 1000°C the observed rise in E was attributed to sintering rather than to the formation of a high modulus new phase.

Loss of Young's modulus is generally attributed to thermal cracking [6, 9–11] but the experimental results are more easily explainable in the following model. Most of the minerals contain hydrated constituents that undergo dehydration upon heating. This decomposition reaction leads to powdered materials of low cohesion and high specific surface A_s that can be measured by nitrogen or krypton adsorption. The physical situation is reminiscent to that described by Clark *et al.* A plausible scenario is sketched on Fig. 2. Qualitatively, variations in Young's modulus can be explained with the help of the minimum surface area [12] or some more sophisticated models. As indicated in the introduction section, the hydrophilic character of a surface can also be varied by chemical treatment. Starting with a gold film deposited on PET by sputtering, Rodhal *et al.* [13] were able to obtain a hydrophilic surface (water contact angle of 5°) by ozone treatment that oxidises the surface or a hydrophobic one (water contact angle of 105°) by methylation. They used Quartz Crystal Microbalance (QCM) to probe the mechanical behaviour of non-rigid, organic layers adsorbed at the solid-liquid interface. By measuring the frequency shift Δf and the attenuation change ΔD during adsorption of the layers, they were able to construct attenuation plots, i.e., ΔD versus Δf curves. These diagrams reveal that adsorption at hydrophobic surface is limited and does not induce large changes in the attenuation D. On the contrary, at ozone-treated surfaces, large changes in D are noticeable. Furthermore, on hydrophilic surfaces, attenuation plot goes through a maximum. They defined the attenuation efficiency of the adsorbed layers as $\frac{\Delta D}{\Delta f}$ and show that this ratio is larger at hydrophilic surfaces than at hydrophobic ones. They came to the conclusion

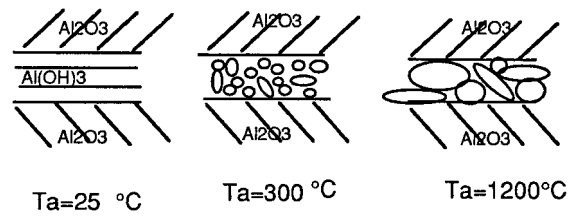

Figure 2 Schematic evolution of gibbsite containing alumina during calcination. Gibbsite dispersed into α alumina is first transformed to powdered material of low cohesion during decomposition at 250°C. The decomposition products sinter at high temperature, leading to coarser grains of large contact area.

that water layers are entrapped at hydrophilic surfaces and that mechanical dissipation takes place inside these layers.

From this literature survey it appears that heat induced cracking of heterogeneous solids is a convenient mean to damage materials. However this damage as measured by the Young's modulus cannot be interpreted as a mere cracking since it exhibits a maximum in the 500°C–800°C range, while the high temperature region is dominated by sintering that increases E. At the same time dehydroxylation leads to a decrease in the damping factor Q^{-1} even when cracking should increase dissipation. The lowering in Q^{-1} and the mass changes associated with changes in E result from a dehydroxylation reaction that needs to be described more precisely. In this paper we present experiments identical to those previously described [1, 2] but in a limited range of temperature where decomposition of gibbsite takes place. Then we perform BET analysis of gibbsite containing products in order to reveal changes in morphology and energetics as induced by annealing up to 1200°C.

3. Experiments

3.1. Zoom in the 150°C–300°C region

As explained in the preceding section, the crack induced lowering of Young's modulus hypothesis is highly questionable. Analysis of the literature shows that lowering of Young's modulus upon heating occurs first in the 250°C–300°C range and is not a linear function of the annealing temperature T_a [4, 9–11]. This decrease is apparent on Figs 12–14 of Ref. [2]. At the same time the damping factor Q^{-1} exhibits a large decrease (see Fig. 11 of the same paper).

The new results presented on Fig. 3 and Fig. 4 are a zoom in the (150°C–300°C) region of the above mentioned ones. It is apparent on Fig. 3 that $E_{(S_w)}$ is not affected by heat treatment before 300°C while on Fig. 4 $Q^{-1}_{(S_w)}$ presents a gradual lowering as soon as 150°C. Also it must be noted that the maximum in the $Q^{-1}_{(S_w)}$ curve at $S_w = 0.1$ is recorded only on the 300°C curve i.e., when $E_{(S_w)}$ starts to decrease. Young's modulus E and damping factor Q^{-1} have also been recorded during adsorption from the laboratory air. Again, results presented on Figs 5 and 6, which are analogous to those presented on Fig. 8 and 10 of Ref. [2] are a zoom in the region of interest. The evolution of $Q^{-1}_{(t)}$ is rather complicated. On a virgin sample (i.e., annealed at 150°C) no change occurs during adsorption. The initial value of Q^{-1} on the 200°C and 250°C curves is high but the most striking result is the decrease in Q^{-1} during adsorption instead of the familiar rise. The usual behaviour i.e., a rise in Q^{-1} upon adsorption is obtained only after a 300°C anneal. Below a 250°C anneal, $E_{(t)}$ exhibits an unexpected large increase upon adsorption (4%). Also, an ordinary situation i.e., a decrease less than 1% during adsorption of water from the laboratory air is not observed before a 300°C anneal.

The main changes induced by annealing are gathered on Table I. These results have been obtained on a

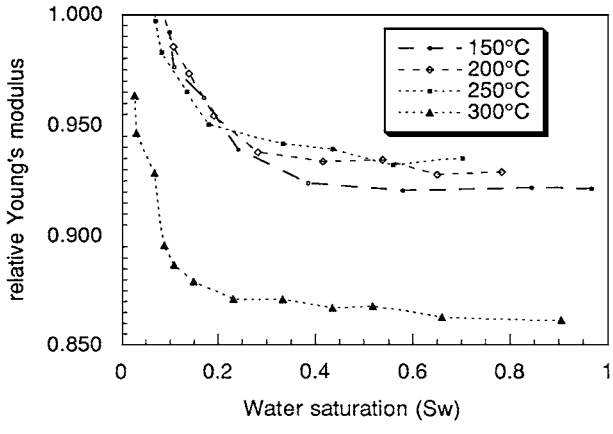

Figure 3 variations of the Young's modulus of gibbsite containing alumina in the 150°C–300°C range.

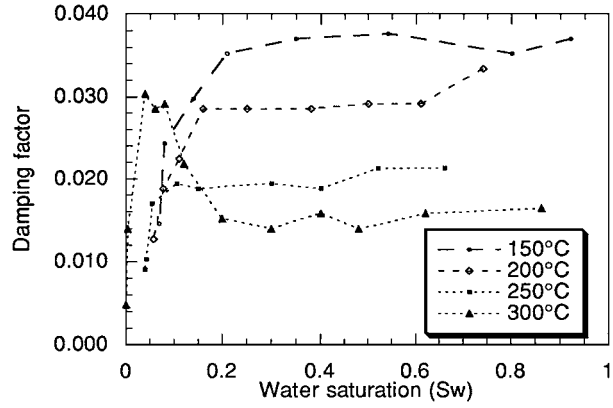

Figure 4 Variations of the $Q^{-1}_{(Sw)}$ of gibbsite containing alumina in the 150°C–300°C range.

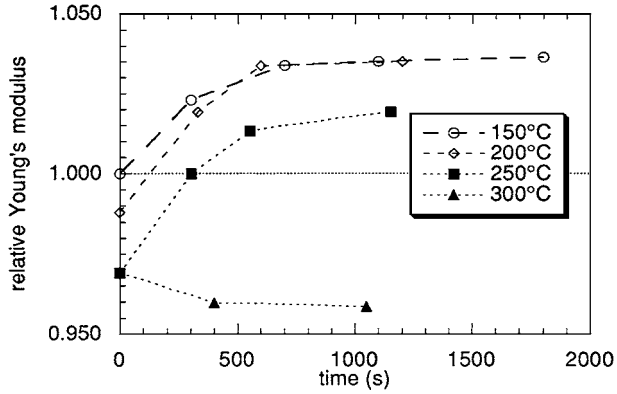

Figure 5 E versus time during adsorption from the laboratory air after annealing at the indicated temperatures.

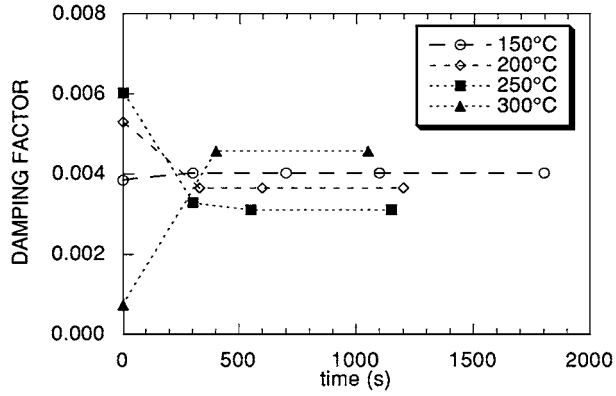

Figure 6 Q^{-1} versus time during adsorption from the laboratory air after annealing at the indicated temperatures.

TABLE I Main parameters affected by heat treatment of gibbsite containing samples

Temperature of annealing (°C)	Mass loss ($\times 10^{-3}$)	Mass gain ($\times 10^{-4}$)	E/E_o	Change in E induced by soaking ($\times 10^{-3}$)	Change in E ($\times 10^{-3}$)	Q^{-1}_{dry} ($\times 10^{-3}$)	Q^{-1} after adsorption ($\times 10^{3}$)	Q^{-1} after soaking (10^{3})	Q^{-1} at the max.
25	0	5.92	1	16	5	2.6	3.5	8.5	Not detected
150	0.12	3.95	0.991	14.3	17.8	2.2	3.5	8.5	Not detected
250	1.97	2.76	0.994	11	42	5.1	2.3	6.0	Not detected
350	5.06	1.58	0.935	16.2	15.5	0.74	1.5	3.9	6.2
500	6.51	1.18	0.899	17.6	9.6	0.36	0.7	1.7	2.8
750	6.75	1.18	0.951	13.2	3.1	0.25	1.2	1.5	4.3
950	6.95	1.18	.955	11.6	1.5	0.40	–	1.3	3.6
1200	6.95	0	0.984	6	−1.5	0.30	0.2	0.5	1.1

single gibbsite containing sample heated at higher and higher temperature up to 1200°C (column 1). The mass losses upon calcination (column 2) are in agreement with the results presented on Fig. 7 of the companion paper [2] and can be attributed to gibbsite decomposition. In column 3, the mass gain upon water adsorption from the laboratory air (RH = 50%) correlates in an inverse fashion with the dehydroxylation as measured by the mass losses upon annealing in column 2. Taking the 25°C and the 1200°C row into account, it can be concluded that a water molecule is adsorbed on two hydroxyls, a result to be compared to the generally accepted value i.e., one physisorbed water molecule per chemisorbed hydroxyl [14]. The results labelled "Young's modulus" presented in column 4 are identical to the ones presented on Fig. 14 of [2]. Large drops in E accompany the gibbsite decomposition at 250°C and also the boehmite → delta alumina transformation at 500°C [15]. The increase in E above 1000°C correlates well with the gravimetric results of columns 2 and 3. At that temperature the hydroxyl coverage goes to zero, this raises the surface energy of the particles, leading to particle coarsening and stiffening of the system according to the minimum surface model of Rice [12] (cf. Fig. 2).

Columns 5 and 6 compare the action upon Young's modulus of water during adsorption from the laboratory air, column 6, (the corresponding gravimetric results are in column 3) and after soaking in liquid water (column 5). As long as the hydroxyl content is noticeable ($T_a < 1000$°C) soaking in water reduces the stiffness of the sample to a large extend. The 1200°C anneal reduces greatly this effect and in this case $E_{(S_w)}$ is a constant. Adsorption from the laboratory air, on the contrary, increases E in a dramatic manner on the 250°C annealed sample. Complete dehydroxylation of the sample at $T_a = 1200$°C leads to opposite behaviour. This is reminiscent of the silica/water couple but on this system the inversion temperature is as low as 400°C [16] that corresponds to the elimination of geminal silanols and it is doubtful that geminal aluminols stand on alumina surface at 1000°C. This change in the state of hydroxylation of the surface induces a lowering in the temperature of desorption of molecular water that reflects the bound to free state transition of adsorbed water as illustrated on Fig. 19 of Ref. [2]. In column 7 Q^{-1}_{dry} is the damping factor of the sample without adsorded water, it exhibits an unexpected peak at 250°C as mentioned above. No clear evolution can be resolved in the 500°C–1200°C range. The mean value in this temperature range, i.e., $Q^{-1} = 3 \times 10^{-4}$ may represent Q_0^{-1} in the expression (2) and stand for intrinsic dissipation, i.e., dissipation due to mechanims other than water adsorption. The results presented on col. 8 duplicate those presented on Fig. 8 of Ref. [2]. On this sample also the 500°C result does not follow the general tendency. The maximum in Column 10, observed near $S_w = 0.1$ [2] follows the general trend, the 500°C point also is erratic and may be related to the boehmite → δ-alumina transformation that occurs at that temperature [15]. However, the general trend is a decrease in the amplitude of the maximum as dehydroxylation proceeds. A full discussion of this maximum is postponed to the third paper of this series.

3.2. BET analysis

The large drop in E that occurs at 250°C has already been encountered by other authors and can be attributed to the hydroxide → oxide decomposition [9, 10]. Thermogravimetic data presented on Fig. 7 of [2] clearly demonstrated that the mass losses of the samples result from the decomposition of gibbsite. This reaction has been followed further by BET analysis of our solid samples used for mechanical tests and of the same gibbsite powder previously used in thermogravimetry.

As in thermogravimetric studies presented in the preceding paper [2], krypton adsorption isotherms at 77 K on hydroxylated samples have been duplicated by blank experiments on powdered pure gibbsite sample purchased from Merck. By routine procedures, the BET specific surface area A_s and the energetic parameter C of the BET equation are obtained. This parameter C is equal to $C = \exp\frac{E_1 - E_L}{RT}$ where E_1 is the heat of adsorption in the first adsorption layer and E_L is the heat of condensation in the bulk liquid phase. This parameter C is of special interest in this study since it has been postulated that mechanical damping of vibrations results from interactions between chemisorbed hydroxyls and bound water physisorbed in the first layer [17, 18]. Tittmann [17] decomposes the loss factor into three terms.

$$Q^{-1} \sim [\text{Total number of active sites}] \times [\text{Volatile mass adsorbed}] \times [\text{Losses in breaking bonds}]. \quad (3)$$

For a given material the first term which is thought to be proportional to the surface area A_s, can be varied

by heating and measured by gas sorption technics. The second one depends on the relative partial pressure of water and in some favourable cases can be measured gravimetrically. Because of its physical meaning, it is expected that the parameter C of the BET equation can stand for the third term in relation (3). The variations in the heat of adsorption E_1 may then reflect the changes in damping efficiency. This is the basis of experiments by Tittmann [17] who measured the damping efficiency of various volatils on the same sample of Coconimo sandstone. According to this author, the difference between water, a high damping fluid, and benzene, a fluid with poor damping capacity, lies in the parameter C since the heat of adsorption of benzene in the first layer is about the same as for liquid adsorbate. In an other publication Tittmann *et al.* produced a curve where the damping efficiency of various fluids (hexane, benzene, ethanol, methanol and water) is plotted against their dipole moment per unit molecular volume [18]. Since this quantity is closely linked to the heat of adsorption, it is expected that C and Q^{-1} are intimately related. The parameter of interest is then the relative polarizability of the substrate and of the adsorbate. In this paper, in contradistinction with the works by Tittmann, we used a single adsorbate (water) and try to vary the polarity of alumina surfaces by performing dehydroxylation/rehydroxylation reactions.

Because of the afore mentioned variability of the raw materials, isotherms have been obtained on an unique sample after annealing at higher and higher temperatures. Typical adsorption isotherms on pure powdered gibbsite are presented on Fig. 7 and Fig. 8 while the corresponding parameters A_s and C are gathered in Tables II and III. Figs 7 and 8 illustrate the huge increase in surface area that occurs in the range 250°C–350°C anneal. The large increase is characteristic of the decomposition process. A large hysteresis loop reflects the small size of the pores that disappears at higher annealing temperature.

In the last rows of Table II and Table III the relative mass losses have been scaled to the maximum losses i.e., 34.6% for the gibbsite powder that corresponds

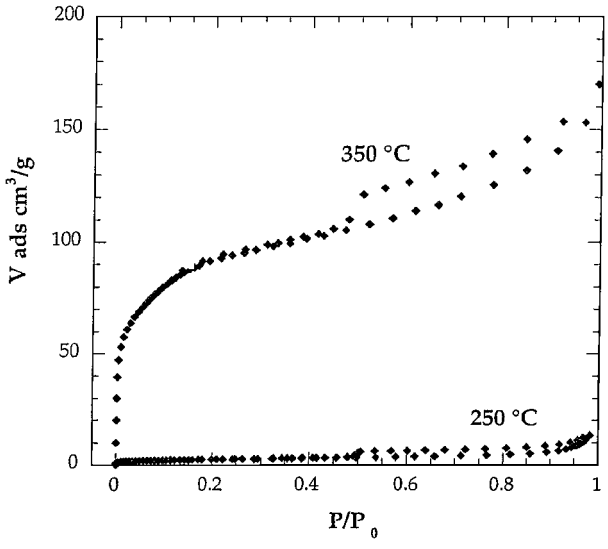

Figure 7 Krypton adsorption isotherm at 77°K on a pure gibbsite sample (Initial-250°C).

TABLE II BET surface area A_s and BET energetic constant C of a gibbsite containing sample used in mechanical experiments as a function of the annealing temperature

Temperature of annealing (°C)	25	250	350	600
BET Surface area A_s (m^2/g)	0.028	0.026	0.044	0.028
BET constant C	7	13	37	40
Relative mass loss (%)	8.4	32.6	62	98.3

TABLE III BET surface area A_s and BET energetic constant C of a gibbsite powder as a function of the annealing temperature

Temperature of annealing (°C)	25	250	300	350	600	850
BET Surface area A_s (m^2/g)	2.7	8.7	369	342	231	119
BET constant C	159	212	135	119	63	97
Relative mass loss (%)	0	5.8	28.2	78.9	96.8	100

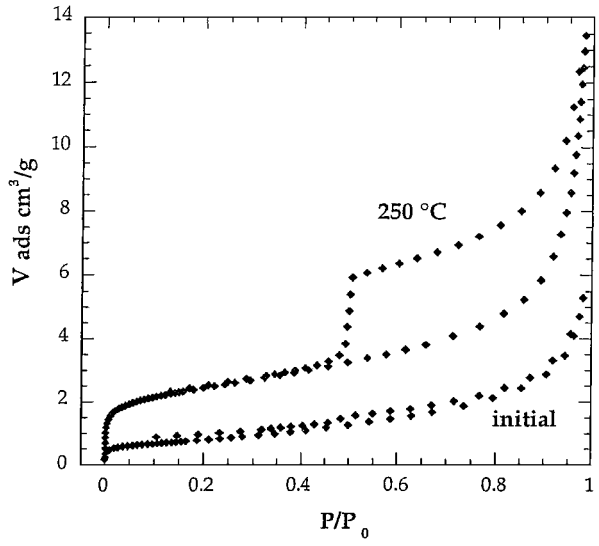

Figure 8 Krypton adsorption isotherm at 77°K on a pure gibbsite sample (250°C–350°C).

closely to the decomposition reaction of gibbsite into alumina. The mass loss of the solid sample (6×10^{-3}) indicates that the mean gibbsite content of the sample is 2% at.

Results presented in these tables are characteristic of a calcination process. At the onset of decomposition the increase in A_s parallels the mass loss curve. It is admitted that the decomposition reaction is a topotactic one i.e., there is no discontinuity between the non transformed parent hydroxide and the newly formed oxide lattices. Increase in surface area results from the recrystallization of the oxide grains which starts at specific sites [19]. The A_s versus T_a curve exhibits a maximum in the 300°C–500°C range. The subsequent decrease in A_s comes from the coarsening of the fine grained structure. Evidences have been afforded that during a dehydration reaction the surfaces of the oxide/hydroxide grains are covered with chemisorbed hydroxyls [19]. During high temperature annealing the OH content of the material decreases in a manner similar to the surface area so that the hydroxyl coverage of the surface grains θ_{OH} varies much more slowly. The driving force for surface area reduction by sintering is the reduction in the total surface energy γA_s where γ is the specific surface energy (J/m^2). It appears that the specific surface energy of oxides is governed by the hydroxyl coverage θ_{OH} [20]. As hydroxyl desorption proceeds, the specific

TABLE IV Alumina: Surface area A_s, water content w and hydroxyl coverage θ_{OH} of alumina obtained by decomposition of a hydrated oxide [19]

Temperature of annealing (°C)	400	600	800	1000
A_s (m^2/g)	300	224	148	99
w ($\times 10^3$)	69	19	12	6
θ_{OH} (monolayer)	1.15	0.4	0.4	0.3

TABLE V Silica : Surface area A_s, water content w and hydroxyl coverage θ_{OH} of silica obtained by decomposition of a hydrated oxide [19]

Temperature of annealing (°C)	200	400	600	800	900
A_s (m^2/g)	715	639	546	397	237
w (x 10^3)	65	40	17.5	5.5	2
θ_{OH} (monolayer)	0.46	0.32	0.16	0.07	0.04

surface energy γ raises, leading to a larger driving force for sintering. The surface energy of oxide is largely dictated by the hydroxyl coverage that remains high at elevated temperature. It has been recently suggested that the hydroxyl coverage governs the $\gamma \rightarrow \alpha$ transformation of alumina and that the γ phase is stabilized against the α transformation by its high hydroxyl coverage [21]. This agrees with the general belief that the surface of oxides obtained by calcination of salts are contaminated by impurities resulting from the decomposition reaction. More precisely the hydroxide coverage on oxide surface is still high after high temperature annealing. Tables IV and V, taken from Gregg [19], illustrate the tendency. The decrease of the surface area reproduces our experimental results and can be attributed to sintering. The decrease in θ_{OH} is much more sluggish on alumina than on silica.

As a closing remark of this paragraph it seems obvious that the choice of the adsorbate is of the utmost importance. Water vapour only probes the hydroxyls on the surface while krypton or nitrogen do not. A more convienent gas would be carbon dioxide that is more polar. Using CO_2 as adsorbate, Lemcoff and Sing [22] found that annealing TK 800 nonporous silica at 1000°C raises C from 4 to 21 and according to Gregg and Sing [23] this can be attributed to a change in polarity of the surface (departure of OH).

As a partial conclusion of the BET analysis and its relation to the present work, it can be said that the observed variations of the BET surface area A_s mirror the changes in the measured Young's modulus. This can be easily explained with the minimum surface modelof Rice [12]. The other goal of this paragraph was to correlate the damping factor Q^{-1} and the energetic BET parameter C as varied by heating. Because of the overwhelming influence of the decrease in the density of adsorption sites (OH sites), it has not been possible to correlate C and Q^{-1} and more precise works are needed here.

4. Discussion

4.1. Interpretation of the results of the literature

The main feature that merges out is the importance of the hydroxyl concentration at the surfaces. As the hydroxyl coverage Θ_{OH} is depleted either by heating or by chemical treatment, the surface turns out to be hydrophobic. This concept help us to interpret the results of Tourenq *et al.* and of Morlier [4, 5]. On minerals hydrophobized by heat treatment, water adsorption reduce the Young's modulus and so the velocity of propagating waves. Clark's results are also easily interpreted if the thermal cracking hypothesis is replaced by the decomposition reaction hypothesis. An aim of this paper was to correlate the BET parameter C and the damping efficiency $Q^{-1}_{(S_w)}$, this correlation is weak because of the lack of results in the 1200°C range where C and Q^{-1} are shown to decline simultaneously. The steady decline in Q^{-1} after annealing at high temperature reflects more the depletion of the hydroxyls (the first term in relation (3)) than a change in the mode of bonding described by the parameter C, the last term in relation (3). Furthermore, the relation between C and Q^{-1} may exhibit a maximum, a low C value implies a weak coupling of the bound water layer to the hydroxyls and a low dissipation but a large value of the parameter C (i.e., strong coupling) would restrict the relative movement and so the dissipation. Since C is measured from non polar gases (i.e., krypton or nitrogen) adsorption, it is not clear how it can reflect polar interactions between the hydroxyls considered as a substrate and an adsorbate (bound water). In our experiments two strongly bonded species have been proved to be inactive in damping. The first ones are the hydroxyls adsorbed on silica. In this case the damping factor at zero bound water coverage does not depend on the hydroxyl coverage, even when it is high [16]. The other ones are oxygenated species on graphite but in this case the oxygen coverage is not precisely known [2].

When bulk hydroxides are present in the solid before heating, the decomposition reaction leads to powdered material inside the sample that decreases the stiffness of the composite. High temperature annealing leads to a coarsening of these crystallites as revealed by the loss of specific surface area A_s and to an increase in E. In these experiments the maximum annealing temperature is still below the sintering temperature of commercial products and E is far from the bulk value.

A plausible route for sintering is the formation of neck between spherical particles as sketched in Fig. 2. The driving force for sintering is the reduction in surface energy γA_S. The higher the surface energy, the higher the driving force for sintering, this explains that sintering takes place only at high annealing temperature after the desorption of hydroxyls that raises the surface energy. It is to be noticed that the rise in E occurs at lower temperature on silica than on alumina, in agreement with the $\theta_{OH}(T)$ presented in Tables IV and V.

An important question still to be discussed is the spatial location of the hydroxyls and we will develop two limiting models. In the first one, a homogeneous, isotropic distribution of the hydroxyls is assumed, it is the H-bonded solid model. In the second one, hydroxyls are located at the inner surfaces of the porous solid and then the behaviour of the sample is dominated by surface interactions, it is the surface energy model. In this second model, a more precise description of the microstructure is needed.

4.2. H-bonded solid model

In order to explain the variations of the Young's modulus of wood as a function of its moisture content, Nissan [24] developed the concept of H-bonded solids. Cohesion of the solid results from bridging the hemicellulose by hydrogen bonding. As hydrogen bonds are sensitive to temperature and to water attack, in such a solid two criteria have to be met

1. The temperature dependence of the Young's modulus is high, $\frac{1}{E}\frac{dE}{dT} = -2 \times 10^{-3}\ K^{-1}$
2. The moisture content of wooden materials affects Young's modulus in a complicated way. Below the fiber saturation point, i.e., in the case of water in the bound state, $\ln \frac{E}{E_o} = -S_w$. Above the fiber saturation point, i.e., in the case of water in the free state, $\ln \frac{E}{E_o} = -6.5 S_w$. Considering an isotropic solid, Nissan derives the following relation for the Young's modulus of a H-bonded solid

$$E = kN^{1/3} \tag{4}$$

where k is the spring constant of the H bond (in the vicinity of 10 N/m) and N is the density of these bonds. In most wood species E lies in the 10 GPa range and application of Equation 4 leads to $N = 10^{27}\ m^{-3}$, a reasonable value.

Y. Kozirovski and M. Folman [25] used a similar model in the case of water vapour adsorbed on Vycor. This simple model can explain the rise in E when water is adsorbed on Vycor from the laboratory air [16]. Here, the rise in E upon adsorption of a water monolayer in the bound state is 1 GPa or $N = 10^{24}\ m^{-3}$. The relative mass change is 3×10^{-2} corresponding to 6×10^{26} molecule H_2O per cubic meter. In other words one water molecule among one hundred is H-bonded to silanols on silica surface. Taking into account the different approximations made, this value is not unreasonable.

4.3. Young's modulus of granular media and surface energy

The concept of H-bonded solid works well in a limited number of situations i.e., water in Vycor for instance but is not operative in the case of alumina. On alumina of surface area $2 \times 10^{-2}\ m^2/g$, the maximum H-bond density on aluminol sites is $10^{23}\ m^{-3}$. The relative change in E upon immersion is as large as 30%, that corresponds to $\Delta E = -30$ GPa. If we suppose that this decrease results from the breaking of H-bonds by attack of molecular water, the spring constant of such bonds would be at least 600 Nm^{-1}, a too large value. So we are led to the conclusion that the mechanical behaviour of our alumina samples is not governed by H-bonding.

Following the seminal work of Johnson *et al.* (JKR theory) dealing with the influence of surface forces on the mechanical properties of divided solids [26], a number of workers have established more precise relations [27, 28]. Considering two spheres of diameter D in contact, because of the van der Waals attraction between the bodies, an attractive force $F = 3/2\pi\Gamma D$ sets in where Γ is twice the surface energy of the solid i.e., the Dupré energy of adhesion. The diameter d of the contact spot is then

$$d = \left[\frac{9\pi\Gamma D^2(1-\nu^2)}{2E}\right]^{1/3} \tag{5}$$

where E is the Young's modulus and ν the Poisson ratio of the material. The elastic deformation under a small applied load P is δ and the contact stiffness $\frac{P}{\delta}$ so that an equivalent Young's modulus can be defined as

$$E^* = \frac{\text{Nominal stress}}{\text{Strain}} = \frac{P}{D^2}\frac{D}{\delta} = \left[\frac{9\pi\Gamma E^2 D^2}{16(1-\nu^2)^2}\right]^{1/3}. \tag{6}$$

This relation allows a measure of the surface energy of solids more reliable than that derived from rupture experiments according to the Griffith formula that is known to overestimate γ because of the plastic work at the edge of the propagating flaw. Checking experimental results against relation (6), Kendall failed in finding a correct order of magnitude of the surface energy of glass beads [27]. As usual in such situations, the discrepancy was attributed to surface contamination but the main interest of relation (6) is the $\gamma^{1/3}$ dependence of E^*. In our experiments the surface energy is expected to vary in three cases.

1. During annealing that leads to dehydroxylation. A literature survey reveals that large variations in γ occur during the dehydroxylation of most of the oxide surfaces [20].
2. During adsorption from the gaseous phase. In this case Gibbs' equation of adsorption links the coverage Γ and the surface energy $d\gamma = -\Gamma d\mu$ where μ is the chemical potential of the adsorbate.
3. During immersion of the solid in liquid water. The relevant parameter is then the heat of immersion q_{imm} that is measured calorimetrically [29].

In the case of Vycor the increase in E^* upon annealing has been attributed to a stiffening of molecular bonds as silanols are converted into siloxane bonds. Kendall *et al.* used the surface energy concept to explain results of this type [27]. As surface energy changes and siloxane bond formation are intimely related both explanations may be considered as valid.

The second case is more complicated. Gibbs' adsorption theorem, coupled with JKR theory would predict a decrease in E^* during adsorption of water vapour from the laboratory air. In our experiments a clear distinction arises among hydroxylated surfaces where E^* raises upon water adsorption and oxane surfaces where E^* decreases. Adsorption on oxane surfaces follows Gibbs' law while it is not obeyed on hydroxylated surfaces. According to this point of view, large positive changes in E^* upon adsorption of minute traces of water vapor are indicative of a highly hydroxylated surface. This is precisely the case on the 250°C annealed, gibbsite containing sample. This agrees with the general belief

that the surface of oxides obtained by calcination of salts are contaminated by impurities resulting from the decomposition reaction [19]. More precisely the hydroxyl coverage on oxide surface is still high after high temperature calcination.

The third situation to discuss is the change in E^* upon immersion, (experimentally the measurements are done during drying) and here also two limiting situations have to be considered. After a 1200°C anneal the $E_{(S_w)}$ curve is rather flat, the ratio $\frac{E(S_w=0)}{E(S_w=1)}$ that characterizes the deleterious action of water is equal to $= 1.05$. On the contrary, after a 250°C anneal that leads to a highly hydroxylated surface, this ratio is equal to 1.60 (cf Fig. 5 of Ref. [1]). In these experiments, the parameter of interest $\Delta\gamma$, may be approximated by the heat of immersion h_{imm}, as measured calorimetrically. It is well known that h_{imm} is strongly dependent on the state of hydroxylation of the surfaces. Experimental values ranging from 130 mJ/m^2 on oxane surfaces to 190 mJ/m^2 on hydroxylated surfaces have been reported [29]. Furthermore, as the absolute value of the surface energy of oxane surface is higher, the relative change in γ, $\frac{\Delta\gamma}{\gamma}$ is much lower on oxane surfaces than on hydroxylated ones. This agrees with the experimentally observed trend i.e., $\frac{E(S_w=0)}{E(S_w=1)} \sim 1$ on oxane surfaces but more quantitative data are not available. For instance Cohen remarked that a usual couple of values can lead to surprising results. Taking 190 mJ/m^2 as the surface energy of (hydroxylated) silica and $h_{\text{imm}} = 260$ mJ/m^2 [30], the surface energy of immersed silica is then negative and the solid would disperse spontaneously in water. However, this situation which is equivalent to $E^* = 0$, has never been observed in the absence of significant dissolution. The $\gamma^{1/3}$ dependence of E^* implies that $\frac{\Delta\gamma}{\gamma} = 3\frac{\Delta E^*}{E^*}$, the maximum relative change in E^* is 30% that corresponds to a 100% change in γ upon immersion, a result that is not unreasonable taking the scattering of the experimental values into account.

To our knowledge, the first experimental verification of the surface energy model has been given by Spencer [31]. He plotted the relative change in Young's modulus ($\frac{E_\infty - E_o}{E_\infty}$ in his notation), against the fractional change in heat of immersion $\frac{\Delta\gamma}{\gamma}$ quoted from other authors, when navajo sandstone is immersed in liquid of various polarity, i.e., water, ethanol and *n*-decane. He obtained a linear plot and concluded that changes in E^* induced by immersion results from unspecified relaxations at the point contacts that involve movement of adsorbed molecules at deformation sites. In other words the diffusivity of adsorbed molecules has to be considered. As an additional proof of the surface energy model Spencer noted that minute amounts of adsorbate reduces E^* as much as full saturation does. Even if the $\gamma^{1/3}$ relationship is not obeyed, the dependence of the Young's modulus on surface energy is clearly established in this work.

5. Conclusion

In this paper, once again, we point out the prominent role of surface hydroxyls on the mechanical behaviour of porous solids during their interactions with water, either in the gaseous or in the liquid phase. Two limiting models have been presented. In the first one the spatial location of the hydroxyls is not specified, the sole parameter taken into account is the density N of the H-bonds. It works well in the case of highly hydroxylated solids when N is larger than 10^{27} m^{-3}. In the second one or surface energy model, the hydroxyls located at the inner surfaces of the solid control the surface energy of the grains into contact. The overall behaviour of the solid is then depicted with the help of JKR theory of divided solids, the main parameter of interest is then the surface free energy γ. The surface energy depends strongly on the hydroxyl coverage and the distinction among the two models may be a mere question of semantics. In this paper a hydroxylated surface is gradually converted to an oxane bond covered surface by heating. At the time the experimental results are more and more closely fitted by the second, surface energy, model. These results agree with those obtained from rupture experiments. In hydrogen bonded systems the Griffith theory is shown not to be applicable, percentage loss in rupture energy as well as percentage loss in Young's modulus are simple functions of the loss of hydrogen bonds [32]. The situation is drastically different on oxane surfaces where interactions are of the van der Waals type, Griffith's theory of fracture and JKR theory of elastic contacts are then applicable.

References

1. J. LEPAGE and J. MENAUCOURT, *J. Mater. Sci.* **33** (1988) 2905.
2. J. LEPAGE, *ibid.* **36** (2002).
3. A. V. KISELEV, in Quart. Rev. Chem. Soc. **XV** (1961) p. 116.
4. C. TOURENQ, B. FOURMAINTRAUX and A. DENIS, in Symposium Soc. Internat. Mécanique des Roches, Nancy (1971) paper I-1.
5. P. MORLIER, *Revue d'Acoustique* **64** (1983) 49.
6. V. A. CLARK, B. R. TITTMANN and T. W. SPENCER, *J. Geophys. Res.* **85** (1980) 5190.
7. R. K. ILER, "The Chemistry of Silica" (John Wiley, New York, 1979) ch. 6.
8. A. R. GREGORY, *Geophysics* **41** (1976) 895.
9. E. NONNET, N. LEQUEUX, P. BOCH, S. L. COLSTON and P. BARNES, *J. Amer. Ceram. Soc.* **84** (2001) 583.
10. N. RICHARD, N. LEQUEUX and P. BOCH, *Key Engineering Materials* **132–136** (1997) 1858.
11. V. A. CLARK, T. W. SPENCER and B. R. TITTMANN, *J. Geophys. Res.* **86** (1981) 7087.
12. R. W. RICE, *J. Mater. Sci.* **31** (1996) 1509.
13. M. RODAHL, F. HÖÖK, C. FREDRIKSSON, C. A. KELLER, A. KROZER, P. BRZEZINSKI, M. VOINOVA and B. KASEMO, *Faraday Discuss.* **107** (1997) 229.
14. A. C. ZETTLEMOYER and H. H. HSING, *J. Colloid Interface Sci.* **58** (1971) 263.
15. J. ROUQUEROL, F. ROUQUEROL and M. GANTEAUME, *J. Catalysis* **36** (1975) 99.
16. J. LEPAGE, A. BURNEAU, G. GUYOT and G. MAURICE, *J. Non-Cryst. Solids* **217** (1997) 11.
17. B. R. TITTMANN, in Proc. IEEE Ultrasonics Symposium (Institute of the Electrical and Electronics Engineers, New York, 1979) p. 327.
18. B. R. TITTMANN, V. A. CLARK, J. M. RICHARDSON and T. W. SPENCER, *J. Geophys. Res.* **85** (1980) 5199.
19. S. J. GREGG, in "The Surface Chemistry of Solids," 2nd ed. (Chapman Hall, London, 1965).
20. G. A. PARKS, *J. Geophys. Res.* **89** (1984) 3997.
21. J. M. McHALE, A. NAVROTSKY and A. J. PERROTTA, *J. Phys. Chem.* B **101** (1997) 603.

22. N. O. LEMCOFF and K. S. W. SING, *J. Colloid Interface Sci.* **61** (1977) 227.
23. S. G. GREGG and K. S. W. SING, in "Adsorption, Surface Area and Porosity" (Academic Press, London, 1982) p. 83.
24. A. H. NISSAN in "Encyclopedia of Materials Science and Engineering," edited by H. M. Bever, p. 2234.
25. Y. KOZIROVSKI and M. FOLMAN, *Trans. Faraday Soc.* **58** (1962) 2228.
26. K. L. JOHNSON, K. KENDALL and D. ROBERTS, *Proc. R. Soc. Lond.* A **324** (1971) 301.
27. K. KENDALL, N. MCN. ALFORD and J. D. BIRCHALL, *ibid.* **412** (1987) 269.
28. C. THORNTON, *J. Phys. D: Appl. Phys.* **26** (1996) 1587.
29. A. C. ZETTLEMOYER and K. S. NARAYAN, in "The Solid-Gas Interface" Vol. 1 (Marcel Dekker, New York, 1967) ch. 6.
30. M. L. COHEN, in Proceeding of the AIP Conference 154, Physics and Chemistry of Porous Media II, Ridgefield, CT, 1986, edited by J. R. Banavar, J. Koplik and K. W. Winkler (American Institute of Physics, New York, 1987) p. 3.
31. J. W. SPENCER, JR, *J. Geophys. Res.* **86** (1981) 1803.
32. P. J. SERADA and R. F. FELDMAN, in "The Solid-Gas Interface," Vol. 2 (Marcel Dekker, New York, 1967) ch. 24.

Received 19 September 2001
and accepted 17 April 2002